

The necessity of maximum information utilization in x-ray analysis

T. Papp^{1,2*}, J. A. Maxwell¹ and A. T. Papp¹

¹Cambridge Scientific, 175 Elizabeth Street, Guelph, ON, N1E 2X5, Canada,

²Institute of Nuclear Research of the Hungarian Academy of Sciences
Bem ter 18/c Debrecen, H-4021, Hungary

Appeared in: X-Ray Spectrometry 38 (2009)3:210-215.

Abstract

There are significant discrepancies in the experimental data needed in the analysis of x-ray spectra. Examination of the data in detail shows that they often contradict simple logic, elemental arithmetic, even parity and angular momentum conservation laws. We have identified that the main source of the problems, other than the human factor, is rooted in the signal processing electronics. We have developed a line of fully digital signal processors that not only have excellent resolution and line shape but also allow proper accounting. We achieve this by processing all events and separating them into two or more spectra where the first spectrum is the accepted or good spectrum and the second spectrum is the rejected spectrum. It is not enough to know that an event was rejected, and increment the input counter, it is necessary to know what and why it happened, whether it was pure noise, a noisy or disturbed event, a true event, or any pile up combination of the above in order to account properly for true event input rate and processor dead time. The data processing methodology cannot be reliably established on the partial and fractional information offered by other approaches. The availability of all the events allows one to see the other part of the spectrum. To our surprise the total information explains many of the shortcomings and contradictions of the x-ray database. We call this a maximum information utilization approach in signal processing. Also a fundamental parameter x-ray fluorescence analysis program (CSX-XRF) has been developed to utilize all the information offered by the signal processor. The fundamental parameter method is only as good as the database it uses and the description of the x-ray fluorescence analysis system. This latter poses significant difficulties, and to ease the demand we have developed an inverse fundamental parameter program package for x-ray tube based equipment characterization.

Cambridge Scientific, 175 Elizabeth Street, Guelph,
ON, N1E 2X5, Canada,

Telephone: (+1) 519-780-1760

Fax: (+1) 519-780-0218

e-mail: tibpapp@cambridgescientific.net

website: www.cambridgescientific.net



Introduction

We have spent significant effort to select the necessary database to use for analytical software for proton induced x-ray emission (PIXE). We have also made x-ray production cross-section measurements for particle impacts. For such measurements it is compulsory to determine the angular distributions of the x-rays [1]. To our surprise it was a very difficult task and yielded very robust data and strong arguments that the general picture of using the independent particle approximation (IPA) is not suitable for the description of the ionisation [2]. However to determine the errors introduced by the IPA model reliable experimental data is necessary. Therefore it is necessary to review the experimental data, on the field where the methodology of energy dispersive detection techniques are used, and all the data related to the x-ray database. We have made a review of the natural line widths based on all available experimental techniques [3], and in the general sense it can be concluded that there are significant weaknesses in the x-ray detection based methods. Such data is necessary for the evaluation of the x-ray spectra [4].

The simplest of measurements are the angular distribution measurements, as the detection efficiency absorptions and all the technical details do not need an absolute determination but it is sufficient to know that they are constant during the measurement. Yet such a methodologically simple exercise has lead to very disturbing results for photoionization, such as strong violation of parity and angular momentum conservation as have been pointed out in [5,6].

The next step in the assessment of the quality of the measured spectra is to look at the relative intensities of the transitions originating from the same initial state. This again does not require absolute measurements. The only available theoretical data is the DF (Dirac-Fock) calculation of Scofield [7]. We do not imply by any means that the Scofield data is the final word on this field as reservations can be raised on several points including that it uses the Babushkin gauge, a self-consistent field model and an IPA. But we can sort the experimental data as to whether they are in close agreement with or strongly deviate from the theory. Some measurements show strong deviation [8,9,10], for which we hope to find a simple explanation. Other measurements give surprisingly and unexpectedly good agreement [11,12] with the Scofield calculation, except for some transitions like $2p_{3/2}-3s_{1/2}$, which are known and expected to deviate to some degree. The main issue here is that the experimental data is not consistent.

To obtain x-ray production cross-sections it is necessary to determine the detector response function and efficiency. The detector response function is a frequently studied subject. One of our reservations is that the signal processing electronics, which has a significant role in the creation of the spectrum, is usually not included in the discussion of the detector response function with a few exceptions [13,5]. Such studies have also yielded some striking results, namely that $K\alpha$ and $K\beta$ or L lines of the same energy have very different tailing at the same x-ray energy [14], which would indicate that there are some fundamental problems to resolve.

In addition to the above complications, we have the issue of fluorescence yields and Coster-Kronig transition probabilities. Examination of the available L shell data shows that they often defy arithmetic and simple scaling laws [15]. The K-shell data is not necessarily any better but the limited information does not offer the same internal consistency check.

Another example is the experimental ionisation cross-sections for particle impacts. They have a large scatter of the order of a factor of three, while each individual measurement accuracy is reported as better than twenty per cent [16]. This implies large unrecognized

systematic errors. One approach that has been used is to take a statistical average of all measurements, although this would yield a wrong value for the physical parameter determined unless by fortuitous circumstance the systematic error yields results that are centered about the true value. Thus we believe that a better approach would be to identify the source of the scatter with the different approaches used, cataloging the different techniques and establishing a correlation that would lead to a better recognition of the systematic errors and thus to better measurements. Using different detectors with their own associated electronics can also be considered “different approaches”.

All of these complications forced us to venture into the field of signal processing electronics and to create a signal processor that basically differs from all existing models in that it is fully digital and processes and collects all events. All signal processors, whether implied or explicitly stated, make use of various discriminators. The presence of discriminators are compulsory as the improved spectrum gives much higher quality that is easier to analyse with much lower limits of detection (LOD), which is clearly advantageous. However if some events are discriminated against and removed from the recorded spectrum we need to know the details of what and why such events were found undesirable so that their absence can be properly accounted for in the spectral analysis. Use of discriminators also opens the possibility of spectrum distortion if the discriminator has some energy dependence. Such an example can be seen in figure 4 of [17]. We have seen such signal processing energy dependence associated with Si(Li) and HPGe detectors as well.

Our original attempt to develop a signal processor yielded improved resolution, improved low energy tailing, better line shape and significant reduction of the pile ups [5,18,19]. However the main aim was to develop a signal processor with the capability to process and display all events (separated into an accepted event and rejected event spectrum) with the rejected events providing enough recognizable information to allow for a quality assurance capability. This created the basis for a more reliable application of the fundamental parameter method for analytical measurements.

In an effort to go beyond the status quo of the field we pursued the idea of using the maximum information available at each level. Processing and storing all events gives additional information at the signal processor level. Depending on the application or the system information being studied the processor creates up to 16 simultaneous spectra with each detected event placed in one or more of the spectra. For the fundamental parameter program we use a Lorentzian line shape that is convoluted with an instrument Gaussian, and furthermore add a detector peak tailing function. We use all x-ray lines for the analysis including pile up lines and pile up with the continuous background. The accuracy of the fundamental parameter method also demands that the description of the experimental conditions be rigorously specified. Working with various XRF equipments based on x-ray tubes we had difficulties in establishing an accurate excitation function at the sample position. This led to the development of an inverse fundamental parameter program package to determine the excitation function that was necessary for a self-consistent analysis.

Quality assurance approach in signal processing.

The task of the signal processor is to create a good quality spectrum. This is a formidable task, as it has to identify all events that include, real events, noise, events with electronic disturbances, events with microphonics, retarded events and any piled up combinations of all these events. If an event is not a true single full energy x-ray event then it is usually advantageous to reject it by using various discriminators. The common method is to

show only this accepted event spectrum but to try to include the rejected event information by incrementing an input event counter. However such an approach does not necessarily provide sufficient information for accurate quantitative analysis, as the disturbances and noise do not follow the same statistical distribution as the true events. They can be much lower, of the same order or much higher than the accepted events but in general are simply unknown for a given measurement.

In our approach we create a minimum of two spectra, one for the accepted events and one for the rejected events. Such spectra can be seen in figure 1 for monochromatized $K\alpha_1$ radiation of Cr. This spectrum was measured with a Si(Li) detector and the Cambridge Scientific CSX4 signal processor.

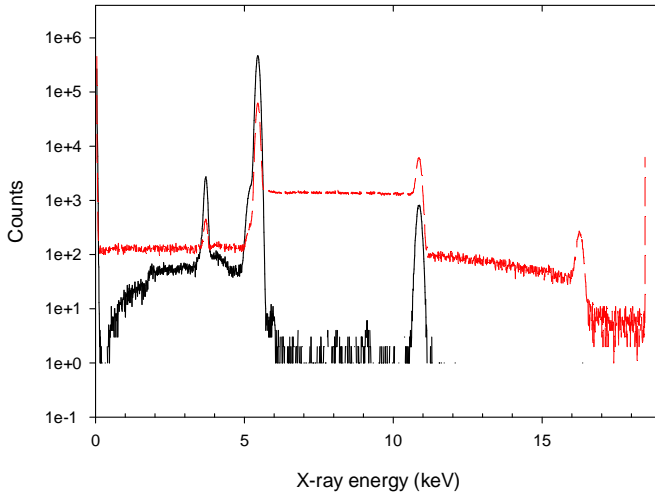


Figure 1. A spectrum of a quasi monochromatized Cr $K\alpha_1$ x-ray peak from an x-ray monochromator is shown. The measured spectrum contains two spectra, one for the accepted spectrum (continuous line) and one for the rejected spectrum (dashed line). The lower side tailing frequently called the plateau, has the expected step at 1.8 keV, demonstrating the excellence. The rejected spectrum allows the analyst to identify the origin of the event, whether it was noise, noisy event, degraded event, electronic disturbance or any combination.

Although a shortened explanation of why the rejected spectrum should look as presented was given in ref [5] a more complete explanation for the appearance of the rejected spectrum for a time variant signal processor is given here. For this particular measurement the signal recognition level was set high to reduce the presence of noise triggered events. This is the reason for the roll off at 1 keV. This discriminator can be set to include or exclude the very low energy regions depending on the analyst's energy range of interest. We were able to observe an escape peak at 60 eV, indicating the capability of the unit to separate the signal from the noise even at these levels. We observe the step at around 1.8 keV as was predicted and explained in [13]. In many systems such a step is not visible being swamped by the noise or pileup of a noise triggered events with real x-rays. The rejected spectrum is generally never seen by the analyst and therefore needs some explanation. The first part of the spectrum from 0 to 5.41 keV is the noise and event pile up. From 5.41 keV to 10.82 keV is the event plus event pile up, that should be counted as two events for a more accurate input rate, as they correspond to two rejected events. From 10.82 keV to 16.2 keV we have the triple event pile up. This region represents three events lost from the accepted spectrum and thus each of these events must increment the event counter thrice and this procedure should continue for higher order pile ups. The last channel is the overflow channel, where all events with energy larger than the selected energy range, as specified by the gain setting, are placed.

Some analysts might not be familiar with the fact that the pile up consists of more than the sum peaks seen in the accepted spectra and therefore a further explanation may be in order. For time variant signal processors the signal recognizer will start the signal shaping procedure. However a second signal could arrive at a later time but within the signal shaping time interval of the first event. Therefore the second signal will contribute to the first event but as it is measured for a shorter time interval and it will contribute with an apparent partial energy. If both signals are real events, then the generated pile up event will contribute to an upper energy plateau. If a signal originating from an E1 energy photon arrives first and within the time period dedicated to an event processing a second signal, originating from a photon of E2 energy arrives and there is no pile up recognition then the pile up will stretch from E1 to E1+E2 energy [20]. This is what we see in the 5.41 keV to 10.82 keV energy range in our case as rejected by the pile up discriminator. It must be emphasized, that for the sum peak we see in the accepted spectrum the two events come very close together in time, usually within the rise time of the pre-amplifier. Completely different methods are used to identify and eliminate the pile up for those situations when the two events arrive within the pre-amplifier rise time, or when the second event arrives at a later time. Therefore it is not possible to determine the overall pile up rate from the sum peak alone without more knowledge or very specific assumptions.

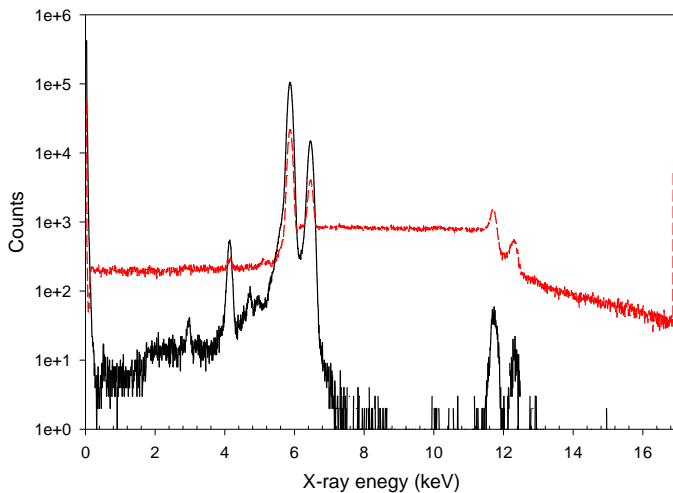


Figure 2. The spectrum of an ^{55}Fe source measured with a Si(Li) detector and the CSX3 signal processor. The signal recognition level was set to 60 eV x-rays. The noise triggered events plateau below the Mn K α peak is much higher compared to that in figure 1 where the signal recognition was set closer to 1 keV. The measured spectrum contains two spectra, one for the accepted spectrum (continuous line) and one for the rejected spectrum (dashed line).

If the signal recognition level is set such that it can be falsely triggered by noise, then the noise event can trigger processing and pile up with an x-ray event and thus contribute to a low energy plateau, e.g. see that part of the rejected spectrum below the Cr K α 1 line in figure 1. At the energy value of E1+E2 is the pile up peak or sometimes referred to as true pile up. It is often called the sum peak as well, with its name inherited from gamma ray spectroscopy. Pile up of noise-triggered events with x-ray events will produce a pile up peak at or near the x-ray line. It is generally assumed that the noise probability distribution is such that it yields a zero mean value, for a long measuring time. However the peaking time interval samples the noise for only a short duration and during this interval the mean of the noise can have a negative or a positive value. Thus the noise signal is not necessarily similar to a photon signal and its recognition by the inspection circuitry or algorithm may not be the same as for two real events indicating that the pile up peak shape may be far from ideal in this case. In actuality many forms are possible that will often manifest as lower and upper energy tailing near the

peak thus contributing to the so called exponential tail on the low energy side or upper energy tailing on the high energy side of the peak. If the signal recognition level is set to a low value, allowing the recognition of low energy events, then the noise triggered plateau will be much higher in the rejected spectrum. Such an example is presented in figure 2.

The impact of pile up on the overall shape of the spectrum strongly depends on the signal processing electronics, and in many cases the detailed knowledge of the signal processor is necessary to evaluate the spectrum. With our processors the extra assumptions are not necessary, as the rejected events spectrum is always available.

We have a series of processors, designed to work with pulsed feedback preamplifiers, with different levels of complexity using two (CSX2), three (CSX3) or four (CSX4) discriminators. In each case the signal processor has a mode where in addition to the accepted and rejected spectra additional spectra are created. The additional spectra are subsets of the rejected event spectrum and show the events rejected by each of the discriminators alone. This can be useful in establishing the proper discriminator values for a particular measurement. Other modes generate additional spectra that can be used to guide the analyst to more robust and reliable measurements. One such spectrum is the arrival time interval between two consecutive events. The dead time and pile up can be determined accurately from the accepted and rejected spectra. However if it is a question whether the incoming x-rays have a normal distribution, or occur in bursts often resulting in an inordinately large amount of pile up for the indicated overall count rate the interval histogram can be useful in answering this question. This allows the analyst to check whether the x-ray source has a different time structure than a random distribution.

Measuring radioactive sources with our processor we were surprised to see the number of degraded events generated by scattered nuclear radiations in the detector that show up in the rejected spectrum [21]. This warrants a reconsideration of the metrology of detector efficiency calibration.

The above analysis presented how the rejected spectrum can be interpreted as pile up of noise and real events with one another. If there is electronic distortion present, it will be visible as a deviation from the flat plateaus. We make use of the rejected spectrum in the fundamental parameter program, where both the accepted rejected spectra are analysed. For each accepted event x-ray line peak a detection system tailing function can be associated. In addition, based on the model presented above, a pile up spectrum is assigned in the rejected spectrum having two rate parameters, one for the x-ray event rate and one for the noise rate. From this assignment the real event rate and the noise event rate are established. Deviation from the presented shape may appear occasionally and those events are assigned as pile up with an electronic disturbance, which is taken into account as well. The processor also counts the preamplifier resets, which along with the preamplifier reset time interval allows calculation of the preamplifier dead time. Each event processed has an associated processing dead time. The processing dead time to first order is the number of processed events multiplied by the calculation dead time. However the processor can make use of the stored signal samples, and if the events are close in time the upper plateau of a signal step can also be used as the lower plateau of the next signal, therefore allowing a higher throughput rate. This is calculated assuming a Poisson distribution and has the effect of reducing the dead time. Our current processors have dead times of the order of a few hundred nanoseconds, and with the typical preamplifier arrangement available with x-ray detectors, this is not a significant issue for input rates up to a few hundred thousand counts per second. After dead time correction the true event input rate (ICR) can be established using information from both the accepted and

rejected spectra. A more detailed description will be presented in forthcoming papers. The importance of the true ICR cannot be over emphasized for accurate analytical work.

The fundamental parameter XRF analysis program.

We have produced a commercially available X-ray fluorescence (XRF) elemental analysis program to take advantage of the extra information that is made available by the Cambridge Scientific line of digital signal processors with the accepted and rejected spectrum. It is a fundamental parameter based code that uses a calibration or correction factor to allow for errors in the system description or the theoretical database. The methods applied are those that have been successfully used in the GUPIX code [22,23] to perform quantitative analysis of PIXE spectra for decades. Much of the X-ray database used is the same as that used with GUPIX with the particle induced X-ray production cross-sections replaced with photon induced production cross-sections. Details of the theoretical database used and the operation of the code will be provided in a later article, however, a brief description will be given below.

The calculation engine code uses input files that contain the X-ray data base information, the spectrum and system description information to estimate element peak areas that in turn are used to estimate element concentrations with the information output to various files for use by the analyst.

In general energy dispersive XRF elemental analysis spectra are comprised of many x-ray peaks superposed on a background of scattered radiation. The signature of each element in the spectrum is one or more series of peaks corresponding to the K, L and/or M X-ray lines and their associated escape peaks. The peak shapes are modeled as Voigtians that result from the convolution of the natural Lorentzian X-ray line shape with the Gaussian instrumental line shape. In addition, parameterized low and high-energy tailing can be associated with each peak. Since every element produces a multi-line signature in the spectrum and each peak if analyzed separately would require several fit parameters to describe it; the X-ray data base is used along with the system description to reduce each series (K,L,M) of lines to a single parameter that is used along with two parameters that convert peak energy to channel position as well as two more parameters that are used to estimate the Gaussian width versus energy over the entire spectrum.

Once the code has determined the peak areas for each element these peak areas are converted to elemental concentration using knowledge of the excitation source, system setup and geometry, the sample composition and areal density, and intervening X-ray absorbers as well as the detector via the following formula:

$$C(Z) = PA(Z) / [H(Z) * Y(Z,E) * Nph(E) * SA * Abs(Z) * Deff(Z)] \quad (1)$$

where $C(Z)$ is the concentration of element Z ; $PA(Z)$ the elemental peak area adjusted for loss due to tailing, pile up and dead time; $Y(Z,E)$ is the theoretical yield of element Z per excitation photon of energy E for the given sample matrix and thickness and specified geometry expressed as X-rays per steradian per exciting photons of energy E per ppm of concentration; $Nph(E)$ is the number of excitation photons of energy E that struck the sample; SA is the solid angle the detector makes with respect to sample in steradians; $Abs(Z)$ is the transmission through any X-ray absorbers between the sample and the detector; $Deff(Z)$ is the detector efficiency of X-rays of element Z (both physical and electronic); and $H(Z)$ is the calibration or correction value that is used to correct the above relation for inaccuracies in the database or

any of the components listed above. For very well characterized systems $H(Z)$ will be approximately one and independent of Z but in general H will be Z or energy and possibly even type (K,L,M) dependent.

The above equation can be extended to multi-line or polychromatic X-ray sources by summing the $Y(Z,E) * Nph(E)$ terms over the list of E values.

There are many details buried in this general description but suffice it to say that accurate analysis depends on an accurate description of each component in the above formula. This is especially true in high-count rate measurements where the peak area corrections for pile up and dead time can become large and information obtained from the rejected spectrum is critical.

In this approach the maximum information utilization is accomplished via using a Voigtian line shape function along with a detector response function, proper dead time and lost event corrections as well as a correction function that allows fine tuning of the database and absorber and detection efficiency corrections for each individual equipment. The program was tested in the x-ray energy range commonly used for RoHS (restriction on hazardous substances) measurements using standards materials of various plastics and alloys.

System calibration program

When an X-ray tube is used as the excitation source in XRF analysis it is critical to know the number of and the energy distribution of the photons striking the sample. This can become especially complicated when primary filters are used to modify the excitation source. In addition, knowledge about the detector crystal thickness and the $H(Z)$ correction factors are also essential for elemental analyses.

In order to facilitate the analysis process we have developed a code that in effect inverts the above formula for determining the elemental concentrations to find the best estimate of the excitation function ($Nph(E)$), detector crystal thickness (part of $Deff(Z)$) and $H(Z)$ values using known concentration values, sample and set-up information.

The primary tube excitation function is assumed to be a Bremsstrahlung spectrum modified by primary filters that also add their own characteristic lines to the excitation spectrum.

The procedure is to collect spectra from one or more standards, use the XRF code to determine peak areas of elements of known concentration then fit excitation parameters and detector crystal thickness until we get the best match between theoretical yields and peak areas with the discrepancy at any given value becoming the $H(Z)$ value. This procedure produces the required excitation function, and matches it with a detector crystal thickness and the appropriate $H(Z)$ values required to analyse samples. Such a typical excitation function is presented in figure 3.

The method was tested on several industrial and laboratory XRF equipments using various standard reference materials, including alloys and plastic materials. Typical results are presented for the polyester based standards of JSAC0611-0615 of the Japanese Society for Analytical Sciences in Table 1. The measurements were made at 50 kV tube voltage for 100 seconds real time for each sample. Measurements have also been made on soil samples where additional sample arrangement techniques were invented to supply further information on the sample thickness and to strengthen the reliability in determination of the invisible elements [24]. A detailed demonstration will be presented in a forthcoming paper. The method worked well in a group of alloys. It also worked well within the group of plastic materials on another industrial collaborator's equipment. It has been tested only with x-ray tubes emitting non-

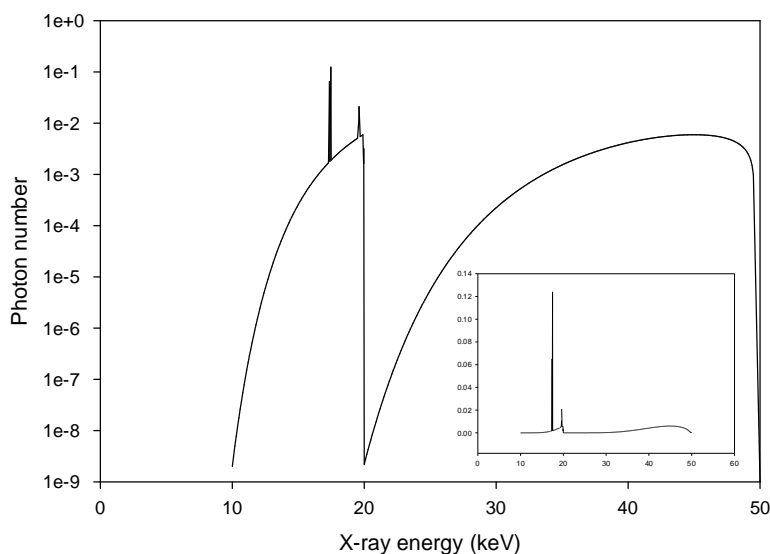


Figure 3. A typical excitation function at the sample position of an XRF system with a tungsten anode and a prefilter package with Mo as the main element. The equipment characterization software package was used for the derivation of the function, using multi element standards.

Sample	Cd (ppm)			PB (L2) (ppm)			Pb(L3) (ppm)		
	ST	Mea-sured	Calc Error	ST	Mea-sured	Calc Error	ST	Mea-sured	Calc Error
JSAC0611	<1	0.9	0.7	<1	1.2	0.6	<1	1.1	0.9
JSAC0612	4.5	5.6	1.0	26.1	28.6	3.1	26.1	26.5	1.5
JSAC0613	10.0	10.4	1.1	54.6	55.8	4.9	54.6	53.7	2.8
JSAC0614	23.8	23.5	1.4	106.8	104.2	3.2	106.8	105.2	3.5
JSAC0615	43.4	43.1	1.7	202.2	201.3	8.3	202.2	203.7	5.7

Table 1. The results of the concentration measurement in polyester based standard samples. The Pb concentration was determined independently from the L2 and L3 subshells' x-rays. The column ST gives the reputed concentration of the elements in the standard materials.

polarized radiation. In general x-ray tube radiation is polarised, with the polarisation of the bremsstrahlung radiation varying within the spectrum as a function of x-ray energy. In such cases the angular distribution of the characteristic and scattered x-rays should be included and there will be strong x-ray tube voltage dependence. As has been presented in the introduction the issue of angular distribution and its significant has not yet been settled with even its obtained sign found to be different by various investigators [25]. Also it is yet to be determined how broad a range of materials can be analysed using the same equipment excitation function. However, before extending the study in this direction we consider it important to make a critical assessment of the fluorescence yields and Coster-Kronig transition parameters, and create a coherent database. Here we put stress on the coherency of the database. With a coherent database the above method will be self-consistent, which is sufficient for industrial and laboratory XRF analysis. With the selected x-ray tubes supplying unpolarised radiation, it was tested at 40 and 50 kV tube voltages. The tube current was

varied over an order of magnitude. The results were satisfactory, and can be attributed to the digital signal processor capability, of reduced pile up, and the availability of rejected event spectrum, thus allowing the determination of a proper true event ICR over a wide counting rate range.

Conclusion

We have developed a line of signal processors that in addition to having very good resolution, line shape and pile up recognition also allows the analyst to accurately determine the real x-ray event input count rate (ICR). It must be emphasized that the recorded or indicated ICR is not the number of x-rays striking the detector but is instead the number of events that trigger the processor. Any disturbance, noise and or pile up that the processor identifies as a trigger event, even if recognized and rejected, is also an event. If the noise and noise pile ups are rejected then the sum of all the noise and event signals, whether accepted or rejected, is the indicated ICR. In real life it is even more complicated because there are not only noises present but also electronic disturbances, and degraded events. Therefore the signal affected by the electronic disturbance is also part of the ICR although a good processor will usually reject it. The indicated ICR is the event counter that is necessary for the dead time calculation but is not necessarily useful in determining the true x-ray event ICR. However the true x-ray event ICR is the value needed in order to determine the events lost from the accepted spectrum due to pile up and distortion and thus allow an accurate rate independent analysis. Analysis of the rejected spectrum along with the accepted spectrum allows us to determine the true number of x-ray events striking the detector within the indicated processor live time and thus provides the basis for the lost event correction. This analysis accounts for noise versus real events and the number of real events in each accepted or rejected pile up event. Without the rejected spectrum it is a demanding task for the analyst to invent a method to estimate the loss of true x-ray events, without making many, possibly unjustifiable, assumptions.

A fundamental parameter XRF analysis software was developed to take advantage of the rejected spectrum, and make the dead time and lost event correction straightforward and automatic. The program uses a maximum information utilization approach, by using Lorentzian line shapes, satellites, and physical description of the detector response function for modelling the x-ray peaks, as well as the information provided by the processor to correct peak areas for dead time and losses.

As the fundamental parameter program demands an accurate description of the system details, it is critical to know the excitation function at the sample position. This is a demanding task, as the x-ray tube and detector properties may change in time. Therefore, the equipment description may be different at the analyst site than was in the factory. The various absorption parameters might not be sufficiently accurate. In order to increase the reliability of the analysis we have developed equipment characterization software where the fundamental parameter program is reversed. Using one or more well characterized standards, the program package can determine the detector efficiency, the correction factors $H(Z)$, and estimate the excitation function at the sample position.

We are in the process of extending the maximum information utilization to the preamplifier stage where we are trying to design a preamplifier that will maximize the information sent to the processor.

Acknowledgements: The preparation of the manuscript was supported by a Marie Curie International Reintegration Grant within the 7th European Community Framework Programme. One of the authors (T.P) is indebted to Prof J.L. Campbell of the University of Guelph, ON, Canada, and Dr. R.G. Lovas of Institute of Nuclear Research of the Hungarian Academy of Sciences, Debrecen, Hungary for their encouragement and support.

References

- [1] T. Papp, Nucl. Instr. and Meth. B 154 (1999) 300-306
- [2] T. Papp, J. L. Campbell and J. A. Maxwell, Phys. Rev. A 48 (1993) 3062
- [3] J. L. Campbell, and T. Papp, At. Data Nucl. Data Tables 77, (2001) 1-56
- [4] T. Papp and J. L. Campbell, Nucl. Instr. and Meth. B 114 (1996) 225
- [5] T. Papp, A.T. Papp and J.A. Maxwell; Analytical Sciences 21 (2005) 737-745
- [6] T. Papp and J. L. Campbell, J. Phys. B: At. Mol. Opt. Phys. 25 (1992) 3765-3770;
A. Tartari, C. Baraldi E. Casnati, A. Da Re, J. E. Fernandez and S. Taioli, J. Phys. B.:
At. Mol. Opt. Phys. 2003, 36, 843, and references therein
- [7] J. H. Scofield 1974 Phys. Rev. A 10 1507 (Erratum 1975 Phys. Rev. A 12 345)
- [8] W Jitschin, G Materlik, U Werner and P Funke, J. Phys. B: At. Mol. Phys. 18 (1985)
1139-1153.
- [9] P.C. Chaves , M.A. Reis , N.P. Barradas and Matjaz Kavcic; Nucl. Instr. and Meth. in
Phys. Res. B 261 (2007) 121-124
- [10] S.J. Cipolla and J. P. Hill, Nucl. Instr. and Meth. in Phys. Res. B 241 (2005) 129
- [11] W. Jitschin, R. Stötzel, T. Papp, M. Sarkar and C. D. Doolen, Phys. Rev. A 52 (1995)
977
- [12] T. Papp, J. L. Campbell and S. Raman, J. Phys. B: At. Mol. Opt. Phys. 26 (1993) 4007
- [13] T. Papp, X-ray Spectrometry 32 (2003) 458-469;
T. Papp, J.L. Campbell, D. Varga and G. Kalinka, Nucl. Instr. and Meth. A 412 (1998)
109
- [14] Van Gysel, P. Lemberge and P. Van Espen, *X-Ray Spectrom.* 2003; 32: 434-441
- [15] http://www.atomki.hu/ar2005/3_atom_mol/a07.pdf, published online
- [16] A. Balsamo, N. De Cesare, F. Murolo, E. Perillo, G. Spadaccini, M. Vigilante, J.
Physics B.: At. Mol. Opt. Phys. 1999, 32, 5699.
- [17] A. Owens, T. Buslaps, C. Erda, H. Graafsma, D. Lumb, E. Welter; NIM A 563 (2006)
268
- [18] T Papp, J.A. Maxwell, A. Papp, Z. Nejedly and J. L. Campbell, Nucl. Instr. and Meth. B
219-220, (2004) 503
- [19] T. Papp, M.-C. Lépy, J. Plagnard, G. Kalinka and E. Papp-Szabó X-Ray Spectrometry.
2005; 34: 106-111
- [20] Statham P. J., X-Ray Spectrometry Vol 6 No2 (1977) p.94;
- [21] Submitted to irma7 conference proceedings, to be published in Applied Radiation and
Isotopes
- [22] J.A. Maxwell, J.L. Campbell and W.J. Teesdale. Nucl. Instr. and Meth. in Phys. Res. B 43
(1988) 218-230.
- [23] J.A. Maxwell, J.L. Campbell and W.J. Teesdale Nucl. Instr. and Meth. in Phys. Res. B 95
(1995) 407-421.
- [24] T. Papp, A.T. Papp, J.A. Maxwell, N. Kawata, T. Utaka and K. Taniguchi; Geophysical
Research Abstracts, Vol.10, EGU2008-A-05161, 2008